Curr Radiol Rep (2018) 6:29
https://doi.org/10.1007/s40134-018-0290-8

PET/CT and Bone Scintigraphy: Metabolic Results in Musculoskeletal Lesions

Rosj Gallicchio[1] · Anna Nardelli[2] · Piernicola Pedicini[1] · Giuseppe Guglielmi[3] · Giovanni Storto[1]

Published online: 3 July 2018

Abstract
Purpose This review aimed to provide an overview on findings from metabolic imaging modalities such as bone scintigraphy and positron emission tomography–computed tomography (PET/CT) in musculoskeletal lesions. It is conceivable that methods assessing metabolism of bone tumors, combined with the morphological assessment, could enhance the possibility for a personalized therapy with particular emphasis to malignant neoplasms.
Recent Findings The assessment of bone tumors by conventional scintigaphic and morphological imaging has been recently integrated with the morpho-metabolic appraisal obtained by PET/CT systems. Increasing availability of this diagnostic modality has been shown to stratify properly the patients and the findings correlate well with outcome. Moreover, new tracers are being implemented in the study of musculoskeletal lesions by PET/CT while the new volumetric parameters used to identify the lesions hold great promise.
Summary Results from PET/CT are associated with tumor grading and histopathology in bone malignant lesions and they could be of value for implementing treatment strategy. Additionally, the metabolic assessment has been demonstrated useful for predicting surgical response and patients' outcome.

Keywords PET/CT · Bone scintigraphy · Musculoskeletal neoplasms · Metabolic findings · Diagnosis and follow-up

Introduction

The assessment of disorders affecting skeleton and muscles relies mainly on morphological imaging. In fact, anatomic imaging procedures including ultrasound, conventional radiography, computed tomography (CT), and magnetic resonance (MR) are commonly used to evaluate malignant tumors, benign neoplasms, and tumor-like lesions for diagnosis, staging, and response to therapy [1, 2]. The morphological evaluation has been considered for a long time the standard for detecting the presence, the size of lesions and therapy response since anticancer cytotoxic agents and surgery make reason of their antitumor activity by determining tumor shrinkage. Surgery and anti-inflammatory regimens perform similarly for the benign tumors. Nevertheless, it is critical to identify reliable diagnostic modalities to follow the size of tumor or benign lesions over time and to determine the degree of response.

In this context, metabolic imaging procedures may provide an added value both in musculoskeletal cancer and non-neoplastic lesions giving reason of diseases' pathophysiology thus tailoring the therapy better. Bone scan (BS) and PET/CT constitute historical and newly introduced imaging modalities for the study of musculoskeletal diseases, respectively. After the introduction of readily available Tc-99m, bone scintigraphy quickly became one of the most common nuclear medicine procedures

This article is part of the Topical collection on *Geriatrics*.

✉ Giovanni Storto
giosto24@hotmail.com

[1] Medicina Nucleare, Istituto di Ricovero e Cura a Carattere Scientifico (IRCCS), Centro di Riferimento Oncologico della Basilicata (CROB), Via P. Pio 1, 85028 Rionero in Vulture, Italy

[2] Istituto di Biostrutture e Bioimmagini, Consiglio Nazionale delle Ricerche (CNR), Naples, Italy

[3] Dipartimento di Radiologia, Università di Foggia, Foggia, Italy

performed to detect skeletal involvement or extra-osseous uptake at least [3]. In particular, the Tc-99m methylene diphosphonate, which demonstrated faster blood-pool clearance than most other Tc-99m labeled diphosphonates, was accepted as the standard agent for skeletal scintigraphy [3, 4]. Based on the advantageous skeletal kinetics of 18F-fluoride, Phelps et al. [5, 6] used 18F-fluoride PET as a model for the evolution of skeletal whole-body PET [7, 8]. PET/CT technology has exhibited higher spatial resolution and substantially greater sensitivity than conventional gamma cameras, resulting in higher image quality for skeletal PET than for the planar bone scintigraphy or SPECT [9, 10]. The increasing availability of PET/CT systems has renewed the interest in using 18F-labeled-NaF as a radiotracer for skeletal imaging since previous technical and logistical limits to its daily usage for bone imaging are no longer present.

Apart from the abovementioned osteotropic tracers, 18F-fluorodeoxyglucose positron emission tomography ([18F]FDG PET/CT) has been established as a suitable tool in tumor assessment and response evaluation of patients suffering from solid tumors who have undergone chemo- and radiotherapy because [18F]FDG reflects the rate of glucose utilization in a tissue (Table 1). It has shown the some value in benign lesions as well [11, 12].

Several studies have demonstrated that treatment-induced changes in lesion [18F]FDG avidity and enduring [18F]FDG uptake after completion of therapies correlated well with patient outcome [13, 14]. Interestingly, as recently observed in hematological diseases, there is emerging evidence that in responding solid neoplasms [18F]FDG uptake decreases significantly in the course of the first chemotherapy cycle, only a few weeks after the beginning of treatment. Although benign musculoskeletal tumors show generally mild uptake as compared to malignancy, their behavior is similar after treatment. On the other hand, when minimal changes in lesion [18F]FDG uptake occur during the early assessment, then a poor patient outcome has to be expected. The abovementioned clinical data support the idea that [18F]FDG PET may be a valuable method to identify responders and non-responders early in the course of therapy and to redirect therapeutic strategies on an individual basis. However, this technique is not yet available for all institutions and several issues should be still addressed such as the most favorable timing in performing metabolic scans, the influence of inflammatory reactions and induced necrosis on image interpretation and the implementation of new radiopharmaceuticals appropriate for molecular imaging.

In a comprehensive morpho-functional approach, a key question is whether it is appropriate to move from anatomic assessment of malignant and benign lesions to volumetric functional assessment with PET or MRI. This review highlights the added value of metabolic imaging for the evaluation of patho-physiology of various musculoskeletal lesions as a valuable supplement to the traditional imaging assessment based only on tumor morphology.

Malignant Bone Tumors

Osteosarcoma

Apart from plasmacytoma, osteosarcoma is the most frequent primary pediatric bone malignancy, with an incidence of approximately 4.8 per million per year that peaks in adolescence [15]. The tumor causes osteolysis with cortical erosion and is associated with a mass in the soft tissues. Macroscopically, osteosarcoma appears as a white–gray mass. Microscopically, bone cells proliferation replace bone marrow forming cartilage, immature bone, and malignant osteoid tissue. This tumor commonly occurs in the distal end of the femur and the proximal ends of the tibia and humerus, and less frequently in the pelvis [16]. Distant metastases frequently arise in the lung parenchyma and bone. Pain may result from stretching of the periosteum, as well as bone destruction and pathologic fracture. Comprehensive imaging, including metabolic imaging, is often helpful at the time of diagnosis and any relapse in order to fully evaluate the extent of disease for appropriate staging, risk stratification and subsequent risk-directed therapy [17]. With dynamic and whole-body Tc-99m-MDP bone scan, lesions show intense vascularity and high concentration in early and blood-pool images, respectively. In the delayed phase, the tracer accumulation is more focal and intense, typically with considerable bony distortion (Fig. 1). Within the area of increased uptake, areas of decreased accumulation (photopenia) may be seen. Nevertheless, in some patients, the accumulation is more defined, uniform, strikingly increased and reflects the findings of the vascular phase. Bone scan can monitor distant recurrence and may demonstrate reduction in the tracer avidity of the tumor after adjuvant chemotherapy, as well as tumor shrinkage. However, its overall accuracy for monitoring therapy is less than MRI [18] and [18F]FDG PET/CT in tumor staging and therapy assessment [19]. 18F-FDG-PET/CT may be mainly useful in the identification of skeletal metastases, given that it has improved sensitivity and specificity as compared to bone scintigraphy [20]. Maximal standardized uptake (SUV_{max}) has been demonstrated to correlate with histological grade making able [18F]FDG PET/CT to differentiate between low and high grade osteosarcoma [21]. Several studies, suggest that changes in the SUV_{max} value can predict histo-pathologic response following neoadjuvant chemotherapy as well as overall survival [22, 23•]. In fact, high SUV_{max} predicts a

Table 1 Summary of recent studies about the potential role of 18F-FDG-PET/CT in musculoskeletal tumors

Study	Year	Neoplasm	Output
Hurley et al.	2016	Osteosarcoma	Better sensitivity and accuracy than bone scintigraphy in the identification of skeletal metastases
Kubo et al.	2016	Osteosarcoma	SUV_{max} values predict the histo-pathologic response and survival after neoadjuvant chemotherapy
Kasalak et al.	2017	Ewings' sarcoma	Better bone marrow assessment than biopsy used routinely in metastatic disease
Hwang et al.	2016	Ewings' sarcoma	SUV_{max} values predict overall survival
Jesus-Garcia et al.	2016	Chondrosarcoma	SUV_{max} value correlates with the grade
Park et al.	2016	Osteoclastoma (giant cell tumor)	Prediction of aggressiveness when the solid component prevails
Boye et al.	2017	Osteoclastoma (giant cell tumor)	Assessment of early response to treatment with denosumab
Dong et al.	2017	Rhabdomyosarcoma	A more confident tool for assigning correctly the M stage
Yamamoto et al.	2014	Liposarcoma	Prognostic value when used prior to therapy

SUV_{max} standardized uptake value

Fig. 1 Bone scintigraphy in osteogenic sarcoma of the distal end of the left femur. The delayed, metabolic images shows intense tracer accumulation that is beginning to affect the surrounding bone

significantly shorter overall survival period than low SUV_{max}. Moreover, [18F]FDG PET/CT had shown high diagnostic accuracy for the detection of recurrences in the follow-up of patients, being it more accurate than conventional imaging [24] and useful for identifying patients who are more likely to be chemotherapy resistant [25].

Ewing's sarcoma

The Ewing's sarcoma is the most aggressive osteogenic pediatric tumor [26]. The overall incidence is 2.93 cases/1000,000 reported annually. This sarcoma has the highest incidence between 5 and 15 years and the proportion of patients with initial distant metastasis remains in the 26 to 28% range. 30–40% of patients will develop local and/or distant recurrent disease typically between 2 and 10 years after the initial diagnosis [27]. The Ewing's sarcoma produces multiple, small, and non-confluent areas of osteolysis whereas the bone structure is completely deleted in the advanced stages. Typically the periosteum reacts in the form of "sheets of onion" and bone spiculae. The invasion of adjacent soft tissues is constant. Macroscopically it appears as a soft white-brown tissue with some hemorrhage. Lymphatic-like cells having a clear cytoplasm are typically aggregated in the so called Homer-Wright rosettes. The tumor takes place in the diaphysis of limbs and in pelvis, frequently in the sacrum. Fever, anemia, leukocytosis, and slimming are present at the clinical onset. The survival of patients is related to the presence of initial metastatic disease (lung or bone marrow), tumor size and to the histologic response after chemotherapy [28]. As a result, a wide-ranging workup is crucial to define the tumor stage including the

lymph node involvement. At dynamic and whole-body Tc-99m-MDP bone scan the Ewing's sarcoma shows considerable hyperemia and high tracer concentration in the blood-pool phase. In the metabolic later images the tracer accumulation is intense but the distribution of uptake is much more homogeneous than osteosarcoma with the bone distortion less marked. Bone scan may show a dramatic reduction in tumor avidity after therapy, in particular it has been demonstrated that changes in the earlier phases of bone scan correlate well with tumor regression. On the other hand, a persistent uptake at ad-interim assessment evokes a poor response. [18F]FDG PET/CT constitutes a valuable method for the staging and follow-up of Ewing's sarcoma [29] and it appears to be of value for the metastatic bone marrow assessment in newly diagnosed Ewing sarcoma. Accordingly, the routine use of blind bone marrow biopsy of the posterior iliac crest can be reconsidered when the FDG-PET/CT is available [30•]. FDG-PET/CT also provides prognostic information irrespective of established prognostic factors in patients with Ewing sarcoma such as age, size, and initial tumor location. SUV_{max} measured by pretreatment [18F]FDG PET/CT can independently predict overall survival in patients with Ewing sarcoma as patients with a $SUV_{max} \leq 5.8$ survived significantly longer than those with a $SUV_{max} > 5.8$ [31]. Salem et al. [32] reported that SUV_{max} obtained with [18F]FDG PET/CT before and after induction chemotherapy can be an indicator of survival in patients with Ewing sarcoma originating in the skeleton. Mean SUV_{max} was 10.74 before (SUV1) and after 4.11 (SUV2) induction chemotherapy, respectively. High SUV1 (HR = 1.05, 95% CI 1.0–1.1, $P = 0.01$) and SUV2 (HR = 1.2, 95% CI 1.0–1.4, $P = 0.01$) were associated with worse overall survival. Interestingly, also newly introduced quantitative [18F]FDG PET/CT parameters, metabolic tumor volume (MTV) and total lesion glycolysis (TLG) have shown value for predicting patients long-term outcome [33].

Chondrosarcoma

Chondrosarcoma is a collective term for a group of malignant tumors that produce atypical cartilage matrix with an infiltrative growth in the bone marrow and cortical bone tissue. However conventional chondrosarcoma accounts for nearly 90% of all chondrosarcomas. The chondrosarcoma can arise de novo or from malignant degeneration of benign cartilage lesions such as enchondromas. Although rare chondrosarcomas represent the second most common primary musculoskeletal malignancy, accounting for approximately 20% of all such tumors. Most patients are 50 years of age or older with a predominance for males. It causes an undefined osteolytic area with cortical bone disruption and moderate periosteal reaction, nevertheless the presence of coarse calcifications within the lesion is crucial for a precise diagnosis. Most of lesion are low-grade tumors, locally aggressive, and non-metastatic, [18]. Macroscopically it appears as a nodular bumped mass involving both the trabecular and cortical bone. Microscopically the hyaline or mixoid aspect is frequently observed. Chondrosarcoma can be classified from grade I to grade III depending on cellularity, atypia, and pleomorphism. The tumor is frequently observed in flat bones particularly sternum, pelvis bones, ribs, and shoulder blades. From a clinical point of view, achy pain, pain at night, nerve dysfunction of the lumbo-sacral plexus or the sciatic, limitation of joint range and pathologic fracture can be encountered. On dynamic and whole-body Tc-99m-MDP bone scan the avidity of tracer is moderately increased within the tumor with scattered focal areas of more intense accumulation, and minimal bony distortion. Even if the bone scintigraphy has the potential for detecting malignization of the benign bone lesions, the findings rarely correlate with histological grading which makes this procedure unconfident when used lone. Accordingly, [18F]FDG PET/CT has recently gained consideration since it can be an important test for identifying chondrosarcomas and their recurrence after surgery [34]. Feldman et al. found the method to have high sensitivity, specificity, and accuracy. They studied the applications of PET/CT in the differential diagnosis between benign and malignant cartilaginous neoplasms thus grading the lesions. In fact, the SUV_{max} was > 3.3 in grade I chondrosarcomas, > 5.4 in grade II and > 7.1 in grade III chondrosarcomas, respectively. They concluded that a SUV value > 2.0 indicated a suspected malignancy [35]. These data were confirmed by Jesus-Garcia et al. [36•] who reported that PET/CT can be used as a quantitative method for differentiating between chondromas and chondrosarcomas located within the long bones. Other authors [37] evaluated the accuracy of PET–CT for predicting the response of chondrosarcomas to treatment and found that the responders showed greater declines in SUV levels as compared to non-responders. These authors concluded that [18F]FDG PET/CT can accurately detect local relapse or metastatic concern.

Chordoma

Chordomas are uncommon tumors that occur from embryonic notochordal remnants along the length of the neuraxis especially at active bone sites.

The chordoma incidence rate was reported to be of 0.08 per 100,000 subjects, was age-dependent, common in males and unusual among patients aged < 40 years [38]. The lesion appears as a destructive lytic lesion, sometimes with marginal sclerosis and expansible soft-tissue mass. The presence of irregular intratumoral calcifications usually correspond to sequestra of normal bone rather than

dystrophic calcifications. Chordomas are locally aggressive, but usually do not metastasize. Macroscopically they appear as a gelatinous mucoid substance associated with hemorrhage and/or necrosis. Chordoma is a slow-growing tumor and symptoms are mainly related to the mass effect on the adjacent structures. The involved sites are the ends of the neuraxis and the vertebral body as well as skull base. Bone scintigraphy has not a role in diagnosis and therapy assessment of chondromas. On the other hand, [18F]FDG PET/CT may play a role in diagnosis, detection of recurrences and choice of treatment option. The tracer uptake has been reported as mild to moderate, sometime heterogeneous, with SUV_{max} values ranging from 2.0 to 5.8. [39–41] The hypoxic component in residual chordomas has been studied by fluoromisonidazole [18F]FMISO PET/CT, a tracer of hypoxia, after surgery and before radiation therapy, in order to tailor the treatment [42].

Osteoclastoma (Giant-Cell Tumor)

The giant-cell tumor, though benign, shows a tendency to local bone destruction, recurrence, malignant transformation and occasionally it metastatizes to the lung and lymph nodes. It represent approximately 5% of all primary bone tumors and 21% of all benign bone tumors and occurs most commonly in the third decade of life with a female predominance [43]. The lesion may appear as an expanding radiolucent neoplasm eccentrically located at the articular surface of long bones. Pathological and histological findings are distinctive with large number of osteoclast-like giant cells in a background of epithelioid cells. The giant cells appear to originate from the fusion of circulating monocytes [44]. Fibroblast-like stromal cells are always present as component of a giant-cell tumor of bone.

Giant-cell tumor occurs at the epiphyses of long bones but it often expands into the metaphysis and frequently arises after the closure of the growth plate. The most common locations are the distal femur, the proximal tibia, the proximal humerus, and distal radius. Clinical symptoms are nonspecific and may comprise local pain, swelling, and limited range of motion of the contiguous joint. At dynamic and whole-body Tc-99m-MDP bone scan the lesion may appear as a “doughnut” in the delayed image and visualized as a ring of increased uptake surrounding an area of reduced uptake. The initial vascularity is characteristically marked and generalized [45]. Although [18F]FDG PET/CT has a role in detecting several malignant bone tumors, benign disease processes may be identified as well. The degree of tracer uptake in a benign giant-cell tumor may be high so that it can be erroneously interpreted as a malignant neoplasm. As a result, it should be always included in the differential diagnosis concerning an intensely [18F]FDG -avid neoplasm [46]. [18F]FDG PET/CT may also reveal a heterogeneous hyper-metabolic lesion with a moderate uptake when the solid components of the tumor prevails on the cystic components, if any [47]. In addition, [18F]FDG PET/CT can be an helpful tool for the evaluation of early response to treatment with denosumab which is a relatively new treatment option for patients with giant-cell tumor of bone [48••].

Malignant Soft Tissues Tumors

Leiomyosarcoma

Leiomyosarcomas are aggressive tumors often difficult to treat that derive from smooth muscle cells typically of gastrointestinal, uterine or soft tissue origin. Those deriving from the soft tissue are thought to occur from the smooth muscle cells coating the small blood vessels. Soft tissue leiomyosarcoma typically is found in adults, nevertheless it can be present in childhood. 50% of all cases of leiomyosarcoma of soft tissue arises in the retroperitoneum, when are involved the deep soft tissues of the extremities they are named leiomyosarcomas of somatic soft tissue. Leiomyosarcoma of bone is extremely rare and affects the metaphysis of long bones and it arises from the smooth muscle cells covering the intraosseous vessels or from pluripotent mesenchymal cells. [49, 50]. In bone, it appears as a typically radiolucent lesion in the metaphysis of a long bone. Leiomyosarcoma of somatic soft tissue has a number of histo-pathologic subtypes such as epithelioid leiomyosarcoma, inflammatory leiomyosarcoma, myxoid leiomyosarcoma, and granular cell leiomyosarcoma.

Symptoms can include weight loss, nausea or vomiting. Leiomyosarcoma of somatic soft tissues, like other soft tissue sarcomas, often is discovered as an enlarging, painless mass. Generally they do not exhibit signs or symptoms of vascular compression while leiomyosarcomas arising from a major blood vessel may cause symptoms of vascular compromise or leg edema and neurologic symptoms. [18F]FDG PET/CT holds some value for biopsy guidance, therapy assessment, and prognostication during the initial staging of soft-tissue sarcomas although its utility needs to be completely defined, [51] (Fig. 2). Definitely, 98% of primary adult soft-tissue sarcomas are FDG-avid and in leiomyosarcoma the SUV_{max} correlates with tumor dimension and tumor grade predicting tumor behavior and almost certainly patient outcome [52].

Rhabdomyosarcoma

Rhabdomyosarcoma is a mesenchymal tumor derived from neoplastic primitive precursor cells. It is a rare soft tissue tumor that can occur at any age, with approximately 500

new cases diagnosed per year in the United States; 41% of cases are reported in adults and 59% in children [53]. Soft tissue sarcomas represent 10% of all childhood malignancies 50% of which are rhabdomyosarcoma. This neoplasm has been recently classified in four subtypes with different histological, genetic, and clinical characteristics: embryonal, pleomorphic, spindle cell/sclerosing, and alveolar [54]. The tumor may arise nearly anywhere in the body but it takes place frequently in the head and neck region. When the tumor is found in the neck, the first sign can be a lump or swelling sometimes associated with pain and redness. Rhabdomyosarcoma can cause the eye to bulge out and can affect the vision as well, or it may provoke earache, headache, or sinus congestion. [18F]FDG PET/CT has been demonstrated helpful for confirming suspicious findings on Tc-99m-MDP bone scan in patients complying with rhabdomyosarcoma diffusely metastatic to the bone marrow [55] and to be more accurate than conventional imaging in the clinical staging and re-staging of patients. The diagnostic accuracies of the T and N stages were similar, whereas [18F]FDG PET/CT correctly assigned the M stage in 89% of patients as compared to 63% of the other modalities [56, 57•]. In addition, [18F]FDG PET/CT has been shown useful in staging and re-staging pediatric rhabdomyosarcoma, especially for the appraisal of lymph nodes and bone involvement, and for detecting unknown primary sites [58]. This methodology could be an additional predictor of outcome and could be used to improve risk-adapted therapy. Baum et al. reported a significantly shorter overall survival in primary tumors visually rated as highly metabolically active or with a ratio of $SUV_{(max)}$ to SUV of the liver above 4.6. Besides, metabolically active lymph node and the presence of metastatic distant sites were indicative of significantly lower survival rates [59].

Liposarcoma

Liposarcoma is a malignancy of fat cells and it is the most common soft tissue sarcoma in adults with a annual incidence of 2.5 cases per million. It accounts for less than 20% of all soft tissue sarcomas. The mean patient age at presentation is 50 years being rare in children. It appears as a large neoplasm, well circumscribed but not encapsulated and can mimic myxoma, lipoma, and cerebral convolutions. Liposarcoma has been classified in three main biologic forms: well-differentiated, myxoid and/or round cell, and pleomorphic. Exceptionally, lesions can exhibit a combination of the different morphologic types. Well-differentiated liposarcoma generally affects deep soft tissues of both the limbs and the retroperitoneum. Myxoid and/or round-cell liposarcomas and pleomorphic liposarcomas have a predilection for the limbs. Rarely it involves the subcutis and skin. Lipoblasts are relatively specific of this neoplasm, look like fetal fat cells and are fairly smaller than mature adipocytes. In general, liposarcoma grows silently and the patient may comply with painful swelling, decreased function, and numbness. [18F]FDG PET/CT has been used for assessing liposarcoma and it has been demonstrated to detect a typical biphasic signal pattern composed of well-differentiated liposarcoma and

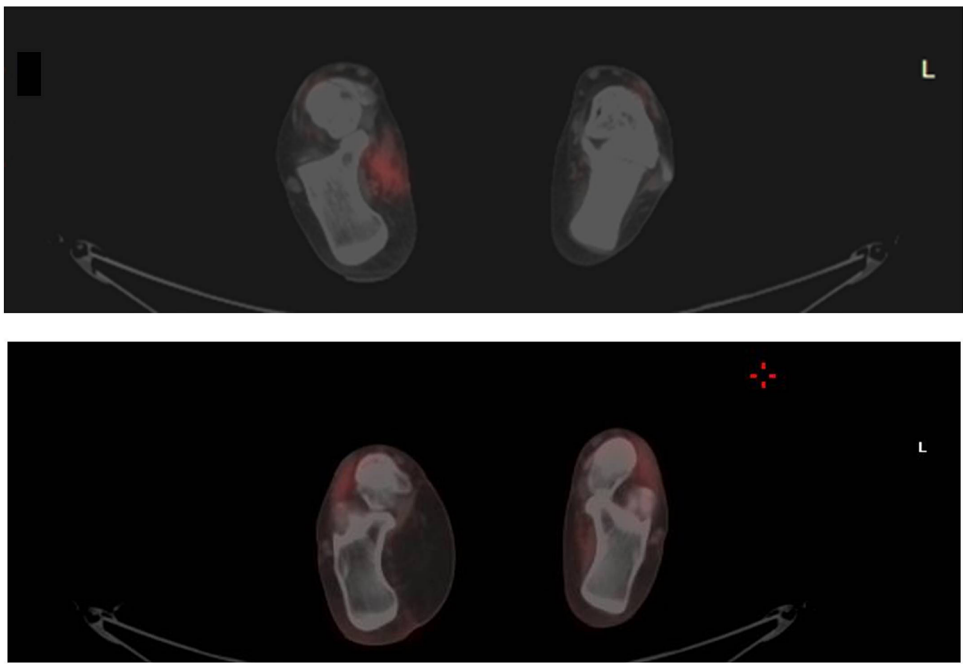

Fig. 2 [18F]FDG PET/CT in a patient complying with leiomyosarcoma of somatic soft tissues of the right foot before (upper) and after (lower) surgical intervention. Note the complete resolution of tracer uptake

dedifferentiated area, that were consistent with the histological grade of malignancy. The uptake value appears to be correlated with tumor grade since well-differentiated and myxoid liposarcomas show mild-moderate uptake whilst high grade neoplasms present a strongly increased uptake [60–62]. [18F]FDG PET/CT has higher sensitivity in detecting osteoblastic metastases in pleomorphic liposarcoma than bone scintigraphy using (99m)TC MDP [63] and it holds value when used prior of therapy providing critical information for the appropriate treatment [64]. Moreover, a SUV_{max} of more than 3.6 resulted in a significantly decreased disease-free survival and stratified patients at high risk for developing early local recurrences or metastatic disease [65].

Benign Tumors

Osteoid Osteoma

Osteoid osteoma is a benign osteoblastic tumor consisting of osteoid component and immature reticular bone tissue. It represents approximately 10% of benign bone tumours, and mostly affects males in the second and third decade [66]. The osteoid osteoma is characterized by a well demarcated subperiosteal osteoid nidus, usually less than 1 cm in diameter and by a surrounding zone of reactive bone formation that can simulate osteomyelitis [67]. Almost 50% of cases affect the metaphysis or proximal diaphysis of the femur, tibia, and omerus [68]. Usually it provokes a severe localized pain worsening at night which is characteristically responsive to prostaglandin inhibitors such as aspirin [69].

Bone scintigraphy is strongly recommended in this context due to its outstanding sensitivity for detecting the presence of osteoid osteoma. In fact, a negative scan virtually excludes the diagnosis whereas an intense focus of uptake within the area of abnormal osteoblastic activity corresponds to the typical osteoma nidus [70]. The valuable role of bone scan is not merely limited to the diagnosis being it frequently needful during the follow-up where a persistent intense uptake correlates with an incomplete excision [71]. [18F-FDG] PET/CT constitutes a complementary, highly sensitive morpho-functional tool that can be used for diagnosis and post-therapeutic evaluation of patients with osteoid osteoma, particularly after the percutaneous radiofrequency ablation [72]. Although it generally exhibit a mild uptake on PET/CT, the osteoid osteoma may show high FDG avidity similar to other malignancies [23•], consequently, a change in FDG uptake can be a consistent indicator of the efficacy after surgery.

Osteblastoma

Osteoblastoma is a rare bone neoplasm closely related to osteoid osteoma, locally aggressive with tendency to involve soft tissues and to transform itself in sarcoma. It is a bone-forming lesion that may affect the cortex, medullary canal, or the periosteal tissues. Osteoblastoma accounts for approximately 1% of all primary bone tumors. in the largest series studied the mean age at presentation was 20.4 years, ranging from 6 months to 75 years [73]. It appears as an ostelytic eccentric area generally covered by periosteum with only a thin rim of bone reaction. The osteoblastoma is composed of several osteoblasts that produce osteoid and woven bone. It commonly involves the vertebral column because approximately 30% of these lesions arise in the spine. Common locations (30%) are also the long bones of the appendicular skeleton while more rarely it involves the pelvic bones, the small bones of the hands and feet, the skull/facial bones, the clavicle, the scapula, and the ribs [74]. The tumor may have a indolent course however the primary symptom is pain, if any. The pain due to osteoblastoma, differently from osteoid osteoma, is not relieved by salicylates. When these tumors develop in the spine, patients may present with neurologic symptoms due to nerve root compression.

Apart from the larger lesion's diameter in osteoblastoma, the role of bone scintigraphy in diagnosis and in response to the therapy is similar to that of osteoid osteoma (Fig. 3). However, the implementation of SPET/CT (tomography) allows a more precise localization of the lesion [75].

As reported by Jeong et al. [76] [18F]FDG PET/CT findings correlate well with bone scintigrapy in the osteoblastoma staging and assessment after surgery. On the other hand, only few studies have demonstrated an exclusive evaluation of osteoblastoma by [18F]FDG PET/CT [77].

Osteochondroma (Osteo-Cartilaginous Exostosis)

Osteochondroma, also called osteo-cartilaginous exostosis or cartilage-capped exostosis, is the most common benign bone tumor. It represents a cartilage-capped bony projection on the external surface of a bone being it solitary or multiple [78]. Osteochondroma accounts for approximately 35% of benign bone tumors and 9% of all bone tumors, with a marked predilection for males and patients younger than 20 years whose epiphiseal cartilages have not yet been consolidated. This cartilage-capped exostosis occurs by means of endochondral ossification during the skeleton development. Macroscopically, it may have a stalk or a broad base of attachment being known as pedunculated and sessile, respectively [79]. Osteochondroma can occur in

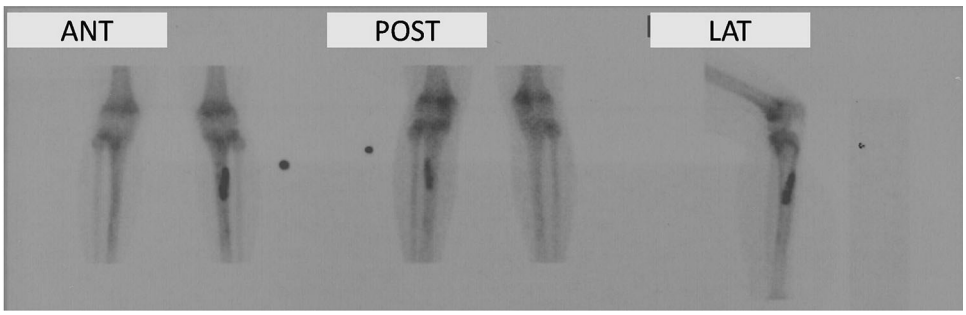

Fig. 3 Bone scintigraphy in osteoblastoma of the tibia. The delayed, metabolic images shows intense focal, well delineated tracer accumulation

any bone site, however it usually affects distal metaphisis of femur and proximal metaphisis of omerus with an asymptomatic course or mild pain. Frequently it is an incidental finding and it is not treated when asymptomatic.

Osteochondroma is a benign chondrogenic tumor, as a result the bone scintigraphy generally shows only a low or absent tracer uptake (Fig. 4). In this context, Kobayashi et al. [80] reported that Technetium-99m DMSA scintigraphy can be superior to Tc-99m HMDP scintigraphy for detecting benign chondrogenic tumors. Even if rarely, the transformation of chondrogenic tumors in chondrosarcoma can be detected [81].

Osteochondroma is only incidentally detected on PET/CT studies, generally shows any or faint FDG uptake well correlating with the metabolic stability of this benign tumor [14, 82].

Enchondroma

Enchondroma constitutes the second common benign bone tumor in young patients without any significant gender bias [83]. It appears as an osteolytic area containing rings of chondroid calcifications with well-defined margins. Most commonly this disorder affects tubular bones, such as metacarpi and phalanxes of hands and feet, in asymptomatic modality. In case of multiple growth plates it is classified as enchondromatosis, (see the Ollier disease and Maffucci syndrome) [84]. On technetium-99m bone scan the images of enchondroma are mostly negative except for the presence of pathologic fractures that imply intense uptake [85]. Generally, if the bone scan results are negative the possibility of a malignancy is extremely remote whereas biopsy is recommended in case of positive findings. The [18F]FDG PET/CT for the evaluation of aggressive cartilage lesions has been reported in small series [40] due to the low uptake of these tumors. In theses settings, as already mentioned, Jesus-Garcia et al. reported a SUV_{max} range from 2.0 to 2.2 with the aim to distinguish enchondroma from other malignancies [41].

Langherans Cell Histiocytosis

Langerhans cell histiocytosis (LCH) is a group of idiopathic disorders characterized by the proliferation of bone marrow–derived Langerhans cells which abnormally accumulate in the involved regions [86]. The LCH estimated annual incidence ranges from 0.5 to 5.4 cases per million persons per year with a male-to-female ratio of 2:1 [87]. LCH encompasses a heterogeneous spectrum of lesions, ranging from a single bone lesion to multi-system involvement. A bone biopsy is often required for the diagnosis in order to rule out other types of diseases, such as metastatic carcinoma, lymphoma/myeloma, osteomyelitis, osteoblastoma, aneurysmal bone cyst and Ewing's sarcoma. In adults with LCH confirmed by biopsy, a chest CT is also needful for detecting the extent of the disease being the lung the most common site of extra-osseous involvement [88]. The most frequent bone sites are

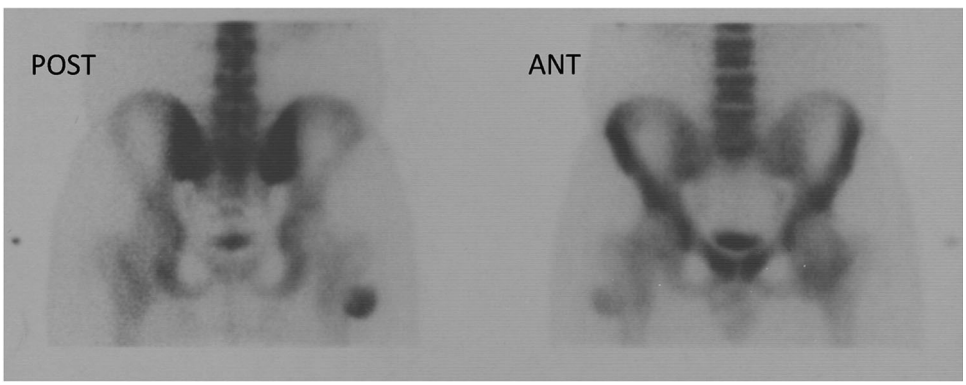

Fig. 4 Bone scintigraphy in osteochondroma (osteocartilaginous exostosis) of the femur. Note the well delineated, moderate tracer uptake

the skull (26%) and jaw (9%), followed by the long tubular bones, pelvis, ribs, and the spine [89]. Clinical features include chronic pain, such as back pain, and fatigue of undetermined etiology. Bone scintigraphy may be a complementary technique to the radiographic skeletal survey in the assessment of bone involvement, but its sensitivity is limited [90]. Noteworthy, [18F]FDG PET/CT constitutes a tool of value for the assessment of both bone and soft tissue involvement (lung, lymphnodes, spleen, or liver) from LCH [91]. This imaging modality can be implemented for LCH diagnosis and treatment response considering that patients with single lesions may respond well to local treatment with an excellent survival, whereas patients with multi-system disease require a more aggressive therapy with a mortality rates that may reach 30 to 40% [92].

Perspectives

New PET/CT Tracers and New Parameters

Musculoskeletal neoplasms may present different biological behaviors. [18F]FDG PET/CT constitutes an established imaging modality for the assessment of musculoskeletal tumors. However, [18F]FDG may present some limitations especially for discriminating benign lesions from soft tissue sarcomas. In this context, the implementation of recent PET radiopharmaceuticals can provide more specific details concerning the biology of musculoskeletal tumors with focus on the tumor grade, treatment monitoring and response [93].

Among the others, the radiolabeled aminoacid, L-3-[18F]-6 α-methyltyrosine (18F-FAMT), can be used as the marker of cell proliferation and of pathological microvessel density within the tumors [94]. Moreover, in this setting a potential imaging agent is the [methyl-11C] choline (11C-choline). The 11C-choline uptake is increased in the musculoskeletal neoplasms cells and it is proportional to the rate of tumor duplication [95] whereas it is negligible in normal bone and soft tissues. Interestingly, the 18F-fluoride can be useful for the evolution of bone metastases and for the estimation of skeletal tumor burden [96].

The proliferation marker [18F]fluorodeoxythymidine (FLT) is available also for the imaging of malignant bone and soft tissue tumors. In fact, FLT uptake correlated significantly with the tumor grade, being it able to evaluate musculoskeletal disease both in staging and treatment response [97].

On PET images the uptake of [18F]galacto-RGD, a biomarker of neoangiogenesis, correlates with the alpha(v)beta3 expression, therefore this tracer might be used for therapeutic targeted regimens with alpha(v)beta3 drugs [98].

Finally, apart from the implementation of new non-FDG tracers, it would be necessary to consider the implementation of volume-based quantitative parameters in daily clinical practice that unlike SUV_{max}, are able to estimate more specifically the tumor burden and to predict patients' outcome and their survival [99, 100].

Conclusions

The metabolic evaluation of musculoskeletal lesions by PET/CT, corroborated by bone scintigraphy when used, is gaining full consideration in diagnosis, staging, therapy assessment and prognostication, especially when combined with morphological modalities such as CT and MRI. Findings from PET/CT correlate well with tumor grading and histopathology and they could be of value for implementing therapeutic strategy. Moreover, the metabolic assessment has been demonstrated useful for predicting histologic response and patients' outcome. This diagnostic modality will provide in a brief delay unique metabolic information due to the implementation in daily routine of new tracers and volumetric parameters.

Compliance with Ethical Guidelines

Conflict of interest Rosj Gallicchio, Anna Nardelli, Piernicola Pedicini, and Giovanni Storto each declare no potential conflicts of interest.

Human and Animal Rights and Informed Consent This article does not contain any studies with human or animal subjects performed by any of the authors.

References

Recently published papers of particular interest have been highlighted as:
- • Of importance
- •• Of major importance

1. Therasse P, Arbuck SG, Eisenhauer EA, Wanders J, Kaplan RS, Rubinstein L, et al. New guidelines to evaluate the response to treatment in solid tumors. European Organization for Research and Treatment of Cancer, National Cancer Institute of the United States, National Cancer Institute of Canada. J Natl Cancer Inst. 2000;92:205–16.
2. Eisenhauer EA, Therasse P, Bogaerts J, Schwartz LH, Sargent D, Ford R, et al. New response evaluation criteria in solid tumours: revised RECIST guideline (version 1.1). Eur J Cancer. 2009;45:228–473.
3. Thrall JH. Technetium-99m labeled agents for skeletal imaging. CRC Crit Rev Clin Radiol Nucl Med. 1976;8:1–31.
4. Davis MA, Jones AG. Comparison of 99mTc-labeled phosphate and phosphonate agents for skeletal imaging. Semin Nucl Med. 1976;6:19–31.

5. Hawkins RA, Choi Y, Huang SC, et al. Evaluation of the skeletal kinetics of fluorine-18-fluoride ion with PET. J Nucl Med. 1992;33:633–42.
6. Raynor W, Houshmand S, Gholami S, Emamzadehfard S, Rajapakse CS, Blomberg BA, et al. Evolving Role of Molecular Imaging with (18)F-Sodium Fluoride PET as a Biomarker for Calcium Metabolism. Curr Osteoporos Rep. 2016;14(4):115–25. https://doi.org/10.1007/s11914-016-0312-5.
7. Hoh CK, Hawkins RA, Dahlbom M, Glaspy JA, Seeger LL, Choi Y, et al. Whole body skeletal imaging with [18F]fluoride ion and PET. J Comput Assist Tomogr. 1993;17:34–41.
8. Grant FD. ^{18}F-fluoride PET and PET/CT in children and young adults. PET Clin. 2014;9(3):287–97. https://doi.org/10.1016/j.cpet.2014.03.004.
9. Schirrmeister H, Guhlmann A, Elsner K, Kotzerke J, Glatting G, Rentschler M, et al. Sensitivity in detecting osseous lesions depends on anatomic localization: planar bone scintigraphy versus 18F PET. J Nucl Med. 1999;40:1623–9.
10. Schirrmeister H, Guhlmann A, Kotzerke J, Santjohanser C, Kühn T, Kreienberg R, et al. Early detection and accurate description of extent of metastatic bone disease in breast cancer with fluoride ion and positron emission tomography. J Clin Oncol. 1999;17:2381–9.
11. Parghane RV, Basu S. Dual-time point 18F-FDG-PET and PET/CT for differentiating benign from malignant musculoskeletal lesions: opportunities and limitations. Semin Nucl Med. 2017;47(4):373–91. https://doi.org/10.1053/j.semnuclmed.2017.02.009.
12. Choi YY, Kim JY, Yang SO. PET/CT in benign and malignant musculoskeletal tumors and tumor-like conditions. Semin Musculoskelet Radiol. 2014;18(2):133–48. https://doi.org/10.1055/s-0034-1371016.
13. Horiuchi C, Taguchi T, Yoshida T, Nishimura G, Kawakami M, Tanigaki Y, et al. Early assessment of clinical response to concurrent chemoradiotherapy in head and neck carcinoma using fluoro-2-deoxy-D-glucose positron emission tomography. Auris Nasus Larynx. 2008;35:103–8.
14. Mac Manus MP, Hicks RJ, Matthews JP, McKenzie A, Rischin D, Salminen EK, et al. Positron emission tomography is superior to computed tomography scanning for response-assessment after radical radiotherapy or chemoradiotherapy in patients with non-small-cell lung cancer. J Clin Oncol. 2003;21:1285–92.
15. Sheikhbahaei S, Marcus C, Hafezi-Nejad N, Taghipour M, Subramaniam RM. PET Value of FDG PET/CT in patient management and outcome of skeletal and soft tissue sarcomas. PET Clin. 2015;10(3):375–93. https://doi.org/10.1016/j.cpet.2015.03.003.
16. Moore DD, Luu HH. Osteosarcoma. Cancer Treat Res. 2014;162:65–92. https://doi.org/10.1007/978-3-319-07323-1_4.
17. Krämer JA, Gübitz R, Beck L, Heindel W, Vieth V. Imaging diagnostics of bone sarcomas. Unfallchirurg. 2014;117(6):491–500. https://doi.org/10.1007/s00113-013-2470-6.
18. Nadel HR. Pediatric bone scintigraphy update. Semin Nucl Med. 2010;40(1):31–40. https://doi.org/10.1053/j.semnuclmed.2009.10.001.
19. Costelloe CM, Chuang HH, Madewell JE. FDG PET/CT of primary bone tumors. AJR Am J Roentgenol. 2014;202(6):521–31. https://doi.org/10.2214/AJR.13.11833.
20. Hurley C, McCarville MB, Shulkin BL, Mao S, Wu J, Navid F, et al. Comparison of (18) F-FDG-PET-CT and bone scintigraphy for evaluation of osseous metastases in newly diagnosed and recurrent osteosarcoma. Pediatr Blood Cancer. 2016;63(8):1381–6. https://doi.org/10.1002/pbc.26014.
21. Rakheja R, Makis W, Skamene S, Nahal A, Brimo F, Azoulay L, et al. Correlating metabolic activity on 18F-FDG PET/CT with histopathologic characteristics of osseous and soft-tissue sarcomas: a retrospective review of 136 patients. AJR Am J Roentgenol. 2012;198(6):1409–16. https://doi.org/10.2214/AJR.11.7560.
22. Harrison DJ, Parisi MT, Shulkin BL. The role of 18F-FDG-PET/CT in pediatric sarcoma. Semin Nucl Med. 2017;47(3):229–41. https://doi.org/10.1053/j.semnuclmed.2016.12.004.
23. • Kubo T, Furuta T, Johan MP, Ochi M. Prognostic significance of (18)F-FDG PET at diagnosis in patients with soft tissue sarcoma and bone sarcoma; systematic review and meta-analysis. Eur J Cancer. 2016;58:104-11. https://doi.org/10.1016/j.ejca.2016.02.007. *This paper highlights the value of SUV_{max} in predicting the histo-pathologic response and survival after neoadjuvant therapy.*
24. Quartuccio N, Fox J, Kuk D, Wexler LH, Baldari S, Cistaro A, et al. Pediatric bone sarcoma: diagnostic performance of ^{18}F-FDG PET/CT versus conventional imaging for initial staging and follow-up. AJR Am J Roentgenol. 2015;204(1):153–60. https://doi.org/10.2214/AJR.14.12932.
25. Palmerini E, Colangeli M, Nanni C, Fanti S, Marchesi E, Paioli A, et al. The role of FDG PET/CT in patients treated with neoadjuvant chemotherapy for localized bone sarcomas. Eur J Nucl Med Mol Imaging. 2017;44(2):215–23. https://doi.org/10.1007/s00259-016-3509-z.
26. Esiashvili N, Goodman M, Marcus RB Jr. Changes in incidence and survival of Ewing sarcoma patients over the past 3 decades: surveillance Epidemiology and End Results data. J Pediatr Hematol Oncol. 2008;30:425–30.
27. McCarville MB, Christie R, Daw NC, Spunt SL, Kaste SC. PET/CT in the evaluation of childhood sarcomas. AJR Am J Roentgenol. 2005;184:1293–304.
28. Lee J, Hoang BH, Ziogas A, Zell JA. Analysis of prognostic factors in Ewing sarcoma using a population-based cancer registry. Cancer. 2010;116:1964–73.
29. Garcia JR, Castañeda A, Morales La Madrid A, Bassa P, Soler M, Riera E. Staging and follow-up of a Ewing sarcoma patient using 18F-FDG PET/CT. Rev Esp Med Nucl Imagen Mol. 2017;26(17):30133–6. https://doi.org/10.1016/j.remn.2017.09.001.
30. • Kasalak Ö, Glaudemans AWJM, Overbosch J, Jutte PC, Kwee TC. Can FDG-PET/CT replace blind bone marrow biopsy of the posterior iliac crest in Ewing sarcoma? Skeletal Radiol. 2017;9. https://doi.org/10.1007/s00256-017-2807-2. *This paper empathizes the importance of PET/CT in replacing bone biopsy when a comprehensive approach is necessary.*
31. Hwang JP, Lim I, Kong CB, Jeon DG, Byun BH, Kim BI, et al. Prognostic Value of SUV_{max} Measured by Pretreatment Fluorine-18 Fluorodeoxyglucose Positron Emission Tomography/Computed Tomography in Patients with Ewing Sarcoma. PLoS ONE. 2016;11(4):e0153281. https://doi.org/10.1371/journal.pone.0153281.
32. Salem U, Amini B, Chuang HH, Daw NC, Wei W, Haygood TM, et al. 18F-FDG PET/CT as an indicator of survival in Ewing sarcoma of bone. J Cancer. 2017;8(15):2892–8. https://doi.org/10.7150/jca.20077 **eCollection 2017**.
33. Amet B, Carlier T, Campion L, Bompas E, Girault S, Borrely F, et al. Initial FDG-PET/CT predicts survival in adults Ewing sarcoma family of tumors. Oncotarget. 2017;8(44):77050–60. https://doi.org/10.18632/oncotarget.20335.
34. Charest M, Hickeson M, Lisbona R, Novales-Diaz JA, Derbekyan V, Turcotte RE. FDG PET/CT imaging in primary osseous and soft tissue sarcomas: a retrospective review of 212 cases. Eur J Nucl Med Mol Imaging. 2009;36(12):1944–51. https://doi.org/10.1007/s00259-009-1203-0.

35. Feldman F, Van Heertum R, Saxena C, Parisien M. 18FDG-PET applications for cartilage neoplasms. Skeletal Radiol. 2005;34(7):367–74. https://doi.org/10.1007/s00256-005-0894-y.
36. • Jesus-Garcia R, Osawa A, Filippi RZ, Viola DC, Korukian M, de Carvalho Campos Neto G, et al. Is PET-CT an accurate method for the differential diagnosis between chondroma and chondrosarcoma? Springerplus. 201629;5:236. https://doi.org/10.1186/s40064-016-1782-8. eCollection 2016. *This manuscript endorses the value of the parameter SUVmax as it correlates with the tumor grade.*
37. Brenner W, Conrad EU, Eary JF. FDG PET imaging for grading and prediction of outcome in chondrosarcoma patients. Eur J Nucl Med Mol Imaging. 2004;31(2):189–95. https://doi.org/10.1007/s00259-003-1353-4.
38. McMaster ML, Goldstein AM, Bromley CM, Ishibe N, Parry DM. Chordoma: incidence and survival patterns in the United States, 1973–1995. Cancer Causes Control. 2001;12(1):1–11.
39. Miyazawa N, Ishigame K, Kato S, Satoh Y, Shinohara T. Thoracic chordoma: review and role of FDG-PET. J Neurosurg Sci. 2008;52(4):117–21.
40. Park SA, Kim HS. F-18 FDG PET/CT evaluation of sacrococcygeal chordoma. Clin Nucl Med. 2008;33(12):906–8. https://doi.org/10.1097/RLU.0b013e31818c4e88.
41. Ochoa-Figueroa MA, Martínez-Gimeno E, Allende-Riera A, Cabello-García D, Muñoz-Iglesias J, Cárdenas-Negro C. Role of 18F-FDG PET-CT in the study of sacrococcygeal chordoma. Rev Esp Med Nucl Imagen Mol. 2012;31(6):359–61. https://doi.org/10.1016/j.remn.2011.11.001.
42. Mammar H, Kerrou K, Nataf V, Pontvert D, Clemenceau S, Lot G, et al. Positron emission tomography/computed tomography imaging of residual skull base chordoma before radiotherapy using fluoromisonidazole and fluorodeoxyglucose: potential consequences for dose painting. Int J Radiat Oncol Biol Phys. 2012;84(3):681–7. https://doi.org/10.1016/j.ijrobp.2011.12.047.
43. Frassica FJ, Sanjay BK, Unni KK, McLeod RA, Sim FH. Benign giant cell tumor. Orthopedics. 1993;16(10):1179–83.
44. Wülling M, Delling G, Kaiser E. The origin of the neoplastic stromal cell in giant cell tumor of bone. Hum Pathol. 2003;34(10):983–93.
45. Oueriagli SN, Ghfir I, Guerrouj HE, Raïs NB. What role for radiobiphosphonates bone scintigraphy in the monitoring of an unusual bone giant cell tumor: a case report and literature review. Am J Nucl Med Mol Imaging. 2016;6(2):128–34.
46. O'Connor W, Quintana M, Smith S, Willis M, Renner J. The hypermetabolic giant: 18F-FDG avid giant cell tumor identified on PET-CT. J Radiol Case Rep. 2014;8(6):27–38. https://doi.org/10.3941/jrcr.v8i6.1328.
47. Park HJ, Kwon SY, Cho SG, Kim J, Song HC, Kim SS, et al. Giant Cell tumor with secondary aneurysmal bone cyst shows heterogeneous metabolic pattern on 18F-FDG PET/CT: a Case Report. Nucl Med Mol Imaging. 2016;50(4):348–52.
48. •• Boye K, Jebsen NL, Zaikova O, Knobel H, Løndalen AM, Trovik CS, et al. Denosumab in patients with giant-cell tumor of bone in Norway: results from a nationwide cohort. Acta Oncol. 2017;56(3):479–83. https://doi.org/10.1080/0284186x.2016.1278305. *The paper is important since it supports the role of metabolic imaging in the assessment of early response to treatment with denosumab.*
49. Berlin O, Angervall L, Kindblom LG, Berlin IC, Stener B. Primary leiomyosarcoma of bone. A clinical, radiographic, pathologic-anatomic, and prognostic study of 16 cases. Skeletal Radiol. 1987;16(5):364–76.
50. Rubin BP, Fletcher CDM. Myxoid leiomyosarcoma of soft tissue, an under recognized variant. Am J of Surg Pathol. 2000;24(7):927–36.
51. Hicks RJ, Toner GC, Choong PF. Clinical applications of molecular imaging in sarcoma evaluation. Cancer Imaging. 2005;5(1):66–72.
52. Punt SE, Eary JF, O'Sullivan J, Conrad EU. Fluorodeoxyglucose positron emission tomography in leiomyosarcoma: imaging characteristics. Nucl Med Commun. 2009;30(7):546–9. https://doi.org/10.1097/MNM.0b013e32832bcaec.
53. Sultan I, Qaddoumi I, Yaser S, Rodriguez-Galindo C, Ferrari A. Comparing adult and pediatric rhabdomyosarcoma in the surveillance, epidemiology and end results program, 1973 to 2005: an analysis of 2,600 patients. J Clin Oncol. 2009;27:3391–7.
54. Kashi VP, Hatley ME, Galindo RL. Probing for a deeper understanding of rhabdomyosarcoma: insights from complementary model systems Nat Rev Cancer. 2015;15(7):426–39. https://doi.org/10.1038/nrc3961.
55. Iagaru A, Goris ML. Rhabdomyosarcoma diffusely metastatic to the bone marrow: suspicious findings on 99mTc-MDP bone scintigraphy confirmed by (18)F-18 FDG PET/CT and bone marrow biopsy. Eur J Nucl Med Mol Imaging. 2008;35(9):1746. https://doi.org/10.1007/s00259-008-0864-4.
56. Tateishi U, Hosono A, Makimoto A, Nakamoto Y, Kaneta T, Fukuda H, et al. Comparative study of FDG PET/CT and conventional imaging in the staging of rhabdomyosarcoma. Ann Nucl Med. 2009;23(2):155–61. https://doi.org/10.1007/s12149-008-0219-z.
57. • Dong Y, Zhang X, Wang S, Chen S, Ma C. 18F-FDG PET/CT is useful in initial staging, restaging for pediatric rhabdomyosarcoma. Q J Nucl Med Mol Imaging. 2017;61(4):438–46. https://doi.org/10.23736/s1824-4785.17.02792-3. *The manuscript report on the value of PET/CT as a valuable tool for determining correctly the M stage.*
58. Ricard F, Cimarelli S, Deshayes E, Mognetti T, Thiesse P, Giammarile F. Additional Benefit of F-18 FDG PET/CT in the staging and follow-up of pediatric rhabdomyosarcoma. Clin Nucl Med. 2011;36(8):672–7. https://doi.org/10.1097/RLU.0b013e318217ae2e.
59. Baum SH, Frühwald M, Rahbar K, Wessling J, Schober O, Weckesser M. Contribution of PET/CT to prediction of outcome in children and young adults with rhabdomyosarcoma. J Nucl Med. 2011;52(10):1535–40. https://doi.org/10.2967/jnumed.110.082511.
60. Nose H, Otsuka H, Otomi Y, Terazawa K, Takao S, Iwamoto S, et al. Correlations between F-18 FDG PET/CT and pathological findings in soft tissue lesions. J Med Invest. 2013;60(3–4):184–90.
61. Hoshi M, Oebisu N, Takada J, Wakasa K, Nakamura H. A case of dedifferentiated liposarcoma showing a biphasic pattern on 2-deoxy-2-f(18)-fluoro-D-glucose positron emission tomography/computed tomography. Rare Tumors. 2013;5(2):95–7. https://doi.org/10.4081/rt.2013.e26.
62. Brenner W, Eary JF, Hwang W, Vernon C, Conrad EU. Risk assessment in liposarcoma patients based on FDG PET imaging. Eur J Nucl Med Mol Imaging. 2006;33(11):1290–5.
63. Yang J, Codreanu I, Servaes S, Zhuang H. Earlier detection of bone metastases from pleomorphic liposarcoma in a pediatric patient by FDG PET/CT than planar 99mTc MDP bone scan. Clin Nucl Med. 2012;37(5):e104–7. https://doi.org/10.1097/RLU.0b013e3182478da8.
64. Yamamoto H, Sugimoto S, Miyoshi K, Yamamoto H, Soh J, Yamane M, et al. The role of 18F-fluorodeoxyglucose (FDG)-positron emission tomography/computed tomography (PET/CT) in liposarcoma of the chest wall. Kyobu Geka. 2014;67(1):4–8.
65. Brenner W, Eary JF, Hwang W, Vernon C, Conrad EU. Risk assessment in liposarcoma patients based on FDG PET imaging. Eur J Nucl Med Mol Imaging. 2006;33(11):1290–5.

66. Xarchas KC, Kyriakopoulos G, Manthas S, Oikonomou L. Hallux osteoid osteoma: a case report and literature review. Open Orthop J. 2017;11:1066–72. https://doi.org/10.2174/1874325001711011066.
67. Xarchas G, Abril JC, Mediero IG, Epeldegui T. Osteoid osteoma with a multicentric nidus. Int Orthop. 1996;20(1):61–3.
68. Sproule JA, Khan F, Fogarty EE. Osteoid osteoma: painful enlargement of the second toe. Arch Orthop Trauma Surg. 2004;124(5):354–6.
69. Laurence N, Epelman M, Markowitz RI, Jaimes C, Jaramillo D, Chauvin NA. Osteoid osteomas: a pain in the night diagnosis. Pediatr Radiol. 2012;42(12):1490–501. https://doi.org/10.1007/s00247-012-2495-y.
70. Sharma P, Mukherjee A, Karunanithi S, Nadarajah J, Gamanagatti S, Khan SA, et al. 99mTc-Methylene diphosphonate SPECT/CT as the one-stop imaging modality for the diagnosis of osteoid osteoma. Nucl Med Commun. 2014;35(8):876–83. https://doi.org/10.1097/MNM.0000000000000134.
71. Infante JR, Lorente R, Rayo JI, Serrano J, Domínguez ML, García L, et al. Use of radioguided surgery in the surgical treatment of osteoid osteoma. Rev Esp Med Nucl Imagen Mol. 2015;34(4):225–9. https://doi.org/10.1016/j.remn.2015.01.003.
72. Imperiale A, Moser T, Ben-Sellem D, Mertz L, Gangi A, Constantinesco A. Osteoblastoma and osteoid osteoma: morphofunctional characterization by MRI and dynamic F-18 FDG PET/CT before and after radiofrequency ablation. Clin Nucl Med. 2009;34(3):184–8. https://doi.org/10.1097/RLU.0b013e3181966de6.
73. Lucas DR, Unni KK, McLeod RA, O'Connor MI, Sim FH. Osteoblastoma: clinicopathologic study of 306 cases. Hum Pathol. 1994;25(2):117–34.
74. Papagelopoulos PJ, Galanis EC, Sim FH, Unni KK. Clinicopathologic features, diagnosis, and treatment of osteoblastoma. Orthopedics. 1999;22(2):244–7.
75. Birchall JD, Blackband K, Freeman BJ, Ganatra RH, O'Leary M, Perkins AC. Precise localisation of osteoblastoma with SPET/CT. Eur J Nucl Med Mol Imaging. 2004;31(2):308.
76. Jeong YJ, Sohn MH, Lim ST, Kim DW, Jeong HJ, Jang KY, et al. Osteoblastoma in the nasal cavity: F-18 FDG PET/CT and Tc-99m MDP 3-phase bone scan findings with pathologic correlation. Clin Nucl Med. 2011;36(3):214–7. https://doi.org/10.1097/RLU.0b013e318208f2f9.
77. Al-Muqbel KM, Al-Omari MH, Audat ZA, Alqudah MA. Osteoblastoma is a metabolically active benign bone tumor on 18F-FDG PET imaging. J Nucl Med Technol. 2013;41(4):308–10. https://doi.org/10.2967/jnmt.113.127332.
78. Giudici MA, Moser RJ, Kransdorf MJ. Cartilaginous bone tumors. Radiol Clin N. Am. 1993;31(2):237–59.
79. Mavrogenis AF, Papagelopoulos PJ, Soucacos PN. Skeletal osteochondromas revisited. Orthopedics. 2008;31(10):1018–28.
80. Kobayashi H, Kotoura Y, Hosono M, Sakahara H, Hosono M, Yao ZS, et al. Diagnostic value of Tc-99m (V) DMSA for chondrogenic tumors with positive Tc-99m HMDP uptake on bone scintigraphy. Clin Nucl Med. 1995;20(4):361–4.
81. Staals EL, Bacchini P, Mercuri M, Bertoni F. Dedifferentiated chondrosarcomas arising in preexisting osteochondromas. J Bone Joint Surg Am. 2007;89(5):987–93.
82. Ishibashi M, Tanabe Y, Fujii S, Ogawa T. Pictorial review of 18F-FDG PET/CT findings in musculoskeletal lesions. Ann Nucl Med. 2017;31(6):437–53. https://doi.org/10.1007/s12149-017-1182-3.
83. Pansuriya TC, Kroon HM, Bovée JV. Enchondromatosis: insights on the different subtypes. Int J Clin Exp Pathol. 2010;3:557–69.
84. Douis H, Saifuddin A. The imaging of cartilaginous bone tumours. I. Benign lesions. Skeletal Radiol. 2012;41(10):1195–212. https://doi.org/10.1007/s00256-012-1427-0.
85. Le BB, Nguyen BD. Ollier disease with digital enchondromatosis: anatomic and functional imaging. Clin Nucl Med. 2014;39(8):375–8. https://doi.org/10.1097/RLU.0000000000000284.
86. Satter EK, High WA. Langerhans cell histiocytosis: a case report and summary of the current recommendations of the Histiocyte Society. Dermatol Online J. 2008;14(3):3.
87. Salotti JA, Nanduri V, Pearce MS, Parker L, Lynn R, Windebank KP. Incidence and clinical features of Langerhans cell histiocytosis in the UK and Ireland. Arch Dis Child. 2009;94(5):376–80. https://doi.org/10.1136/adc.2008.144527.
88. Haupt R, Minkov M, Astigarraga I, Schäfer E, Nanduri V, Jubran R, et al. Langerhans cell histiocytosis (LCH): guidelines for diagnosis, clinical work-up, and treatment for patients till the age of 18 years. Pediatr Blood Cancer. 2013;60(2):175–84. https://doi.org/10.1002/pbc.24367.
89. Satter EK, High WA. Langerhans cell histiocytosis: a review of the current recommendations of the Histiocyte Society. Pediatr Dermatol. 2008;25(3):291–5. https://doi.org/10.1111/j.1525-1470.2008.00669.x.
90. Goo HW, Yang DH, Ra YS, Song JS, Im HJ, Seo JJ, et al. Whole-body MRI of Langerhans cell histiocytosis: comparison with radiography and bone scintigraphy. Pediatr Radiol. 2006;36:1019–31. https://doi.org/10.1007/s00247-006-0246-7.
91. Obert J, Vercellino L, Van Der Gucht A, de Margerie-Mellon C, Bugnet E, Chevret S, et al. 18F-fluorodeoxyglucose positron emission tomography-computed tomography in the management of adult multisystem Langerhans cell histiocytosis. Eur J Nucl Med Mol Imaging. 2017;44(4):598–610. https://doi.org/10.1007/s00259-016-3521-3.
92. Monsereenusorn C, Rodriguez-Galindo C. Clinical Characteristics and Treatment of Langerhans Cell Histiocytosis. Hematol Oncol Clin North Am. 2015;29(5):853–73. https://doi.org/10.1016/j.hoc.2015.06.005.
93. Wieder HA, Pomykala KL, Benz MR, Buck AK, Herrmann K. PET tracers in musculoskeletal disease beyond FDG. Semin Musculoskelet Radiol. 2014;18(2):123–32. https://doi.org/10.1055/s-0034-1371015.
94. Jager PL, Vaalburg W, Pruim J, De Vries EGE, Langen KJ, Piers DA. Radiolabeled amino acids: basic aspects and clinical applications in oncology. J Nucl Med. 2001;42(3):432–45.
95. Hara T, Inagaki K, Kosaka N, Morita T. Sensitive detection of mediastinal lymph node metastasis of lung cancer with 11C-choline PET. J Nucl Med. 2000;41(9):1507–13.
96. Lapa P, Marques M, Costa G, Iagaru A, Pedroso de Lima J. Assessment of skeletal tumour burden on 18F-NaF PET/CT using a new quantitative method. Nucl Med Commun. 2017;38(4):325–32. https://doi.org/10.1097/MNM.0000000000000654.
97. Buck AK, Herrmann K, Büschenfelde CM, Juweid ME, Bischoff M, Glatting G, et al. Imaging bone and soft tissue tumors with the proliferation marker [18F]fluorodeoxythymidine. Clin Cancer Res. 2008;14(10):2970–7. https://doi.org/10.1158/1078-0432.CCR-07-4294.
98. Beer AJ, Haubner R, Sarbia M, Goebel M, Luderschmidt S, Grosu AL, et al. Positron emission tomography using [18F]Galacto-RGD identifies the level of integrin alpha(v)beta3 expression in man. Clin Cancer Res. 2006;12(13):3942–9.
99. Li YJ, Dai YL, Cheng YS, Zhang WB, Tu CQ. Positron emission tomography (18)F-fluorodeoxyglucose uptake and prognosis in patients with bone and soft tissue sarcoma: a meta-analysis. Eur J Surg Oncol. 2016;42(8):1103–14. https://doi.org/10.1016/j.ejso.2016.04.056.

100. Andersen KF, Fuglo HM, Rasmussen SH, Petersen MM, Loft A. Volume-Based F-18 FDG PET/CT Imaging Markers Provide Supplemental Prognostic Information to Histologic Grading in Patients With High-Grade Bone or Soft Tissue Sarcoma. Medicine (Baltimore). 2015;94(51):e2319. https://doi.org/10.1097/MD.0000000000002319.